

# Design strategies for the creation of aperiodic nonchaotic attractors

Amitabha Nandi<sup>1</sup>, Sourav K. Bhowmick<sup>2</sup>, Syamal K. Dana<sup>2</sup> and Ram Ramaswamy<sup>3</sup>

<sup>1</sup>*Max-Planck Institut für Physik Komplexer Systeme, Nöthnitzer Str. 38 01187 Dresden, Germany*

<sup>2</sup>*Instrument Division, Indian Institute of Chemical Biology, Kolkata 700 032, India*

<sup>3</sup>*School of Physical Sciences, Jawaharlal Nehru University, New Delhi 110 067, India*

Parametric modulation in nonlinear dynamical systems can give rise to attractors on which the dynamics is aperiodic and nonchaotic, namely with largest Lyapunov exponent being nonpositive. We describe a procedure for creating such attractors by using random modulation or pseudo-random binary sequences with arbitrarily long recurrence times. As a consequence the attractors are geometrically fractal and the motion is aperiodic on experimentally accessible timescales. A practical realization of such attractors is demonstrated in an experiment using electronic circuits.

PACS numbers: 05.45-a

**Generating dynamics which is aperiodic, but nevertheless stable in a sense that nearby trajectories coalesce and synchronize, has been of considerable interest in the past few years. Such motion has been typically observed in driven dynamical system, in particular when the drive is quasiperiodic. Since quasiperiodicity is difficult to achieve in practice, a major issue in this regard has been whether such dynamics can be achieved by other techniques, and has been answered with various degrees of success. Here we present a simple design scheme that uses pseudo-random binary sequences with very long recurrence times to switch the dynamics between two different states. The resultant dynamics goes to an attractor which is aperiodic and stable, namely has negative Lyapunov exponent. Characterization of such dynamics reveals the fractal nature of such dynamics and also their differences with the ones obtained by quasiperiodic drive. Such a design scheme is further realized in an experimental setup using electronic circuits, suggesting potential applications in practical situations.**

## I. INTRODUCTION

The design of dynamical systems in which the motion is both aperiodic and stable has been an objective of a number of recent studies [1]. One realization of this goal is in strange nonchaotic attractors (SNAs) that can be created in quasi-periodically driven systems [1, 2]. In such systems which have been known for over twenty years now [3], the attractor has a fractal geometry, and this results in the dynamics being aperiodic. The Lyapunov exponents of the drive system are nonpositive: this lead to a lack of sensitivity to initial conditions, and thus to the synchronization of orbits [4].

Achieving quasiperiodicity is simple in principle, but

difficult in practice. Quasiperiodic modulation requires that the system be driven either through a single source that has an irrational frequency (for maps), or with two sources whose frequencies are incommensurate (for flows). Experimental uncertainties are usually larger than the precision with which rational or irrational numbers can be measured, and therefore finding or creating SNAs in practical situations has proved to be difficult, except for isolated experiments [5]. If strange nonchaotic dynamics is to be taken seriously, it is necessary to ask if such behaviour can arise in the absence of strict quasiperiodicity. In particular, most physical, biological and engineering systems will not be quasiperiodic, so it is natural to ask whether SNAs can arise in situations where the underlying system is autonomous, or has other time dependence.

Earlier studies have addressed this issue [6, 7, 8, 9] with varying degrees of success. The use of an external noise source typically has the effect of smearing out attractor structure and gives effective Lyapunov exponents that are nonnegative. As a result the dynamics is neither truly strange nor truly nonchaotic [10]. The recent suggestion by Wang *et al.* [9], that additive noise alone can be used to induce robust SNAs in both maps and flows appears to ensure that the attractors so created share the mathematical properties of SNAs formed by other bifurcation routes [1, 9].

The approach taken in the present paper pursues a different route. We show that by using parametric modulation based on deterministic pseudorandom dynamics, it is possible to create dynamical attractors that are stable, nonchaotic and aperiodic, and which will appear strange on any measurable timescale. In this context the term ‘strangeness’ refers purely to the geometry, while stability refers to the fidelity in signal reproduction or tracking [11], an issue that, for instance, underlies schemes for encryption and communication.

Our procedure for the creation of such aperiodic nonchaotic attractors (ANAs) relies on the use of binary random numbers to modulate the dynamical system between two dynamical states, a stable fixed point and a chaotic

attractor. By suitably designing the drive dynamics, it is possible to ensure that the asymptotic dynamics of the driven system has (a) a negative largest Lyapunov exponent, and (b) nontrivial and complicated geometry on spatial scales that are determined by the (essentially) experimental resolution. We show that such attractors can be created in both discrete-time autonomous maps as well as flows, and further present an experiment based on electronic circuits to support our findings. This suggests that ANAs could have potential application in practical situations where aperiodic dynamics is desirable, as for example in chaotic communications. At the same time, these attractors have differences from those created by quasiperiodic driving and other methods [1, 2]. It should be noted that dichotomous driving has been used before in both numerical [12] as well as experimental [13] studies, although the motivation there was to study noise-induced transitions between different states or attractors.

In the following section we discuss the design of ANAs in the driven Hénon map and the driven Lorenz system using a deterministic feedback shift register to generate a pseudorandom drive [1]. In Sec III we discuss similar driving mechanism using chaotic sequence from a Chua circuit. The study of such attractors and their proper characterization is discussed in Sec IV, where we show the geometric differences between ANAs and comparable SNAs. In Sec V we present an experimental realization of such attractors using electronic circuits, and conclude in Sec VI with a discussion and summary of our results.

## II. DICHOTOMOUS DETERMINISTIC MODULATION

Consider a dynamical system (with one freedom and a single parameter for simplicity, but with obvious extension to higher dimensions and to the case of several parameters)

$$x \rightarrow f(x, b), \quad (1)$$

that is modulated through the output of a binary drive sequence (strings of 0's and 1's)  $z_n$  as

$$x_{n+1} = f(x_n, b_1 + z_n(b_2 - b_1)). \quad (2)$$

Depending on the value of  $z_n$ , the system parameters thus switch between  $b_1$  and  $b_2$ , giving a dichotomous modulation that is, nevertheless, deterministic.

One standard way of achieving this is to use a linear feedback shift register (LFSR)[14] that generates a pseudo-random bit sequence  $\{z\}$  through a delay mapping of the general form

$$z_{n+1} = \sum_{i=1}^N a_i z_{n+1-i} \quad \text{mod } 2, \quad (3)$$

where  $a$  is also a binary variable. For a specific choice of nonzero  $a$ 's for a given  $N$  (the ‘‘tap sequence’’), the dynamics is on an attractor with period  $\leq 2^N - 1$ . The analog generalization (namely, the analog feedback shift registers (AFSR)) [15] uses the same coefficients in a continuous mapping

$$z_{n+1} = \frac{1}{2} - \frac{1}{2} \cos \pi \sum_{i=1}^N a_i z_{n+1-i}, \quad (4)$$

to generate a pseudorandom sequence of 0's and 1's. This dichotomous drive is, importantly, a dynamical system and the drive sequence is an *attractor* of the dynamics. The sequence is optimal if arbitrarily long sequences of either 0 or 1 occur. The theory of LFSRs (and thus of AFSRs) is well-developed and minimal tap sequences that produce the longest possible (namely  $2^N - 1$ ) period pseudorandom sequences are easily available [14]. For sufficiently large  $N$ , the period of the pseudorandom sequence can quickly exceed the age of the universe at any realistic sampling rate.

Designing aperiodic but nonchaotic dynamics in  $x$  is straightforward: for instance if  $b_1$  corresponds to a case of, say, superstable dynamics, and  $b_2$  to the case of chaotic dynamics in the system (Eq. 2), the resultant dynamics in the driven system will be aperiodic but will rapidly be attracted to the superstable orbit whenever there is a ‘‘gap’’, namely a string of 0's. The Lyapunov exponent will consequently be negative and as a result trajectories with arbitrary initial conditions will synchronize.

Special attention should be given when choosing the tap sequence  $N$ . It must be large enough such that the recurrence time, namely  $2^N - 1$  is much longer than the time-scales used for simulations. For smaller  $N$ , the recurrence also become short, and since the AFSR dynamics is periodic, the system dynamics will go to a periodic attractor.

Any other random sequence will also serve the purpose, but LFSRs or AFSRs offer a practical advantage over other pseudo random number generators (PRNGs). The shift registers are maximally stable [15]: being attractors of the dynamics their stability and controllability—unlike that of stochastic sequences or PRNGs—is more easily ensured. Furthermore, since feedback shift registers are dynamical systems as well, the entire drive–response system can be represented as a delay dynamical system.

We discuss representative examples below.

### A. Hénon Map

The Hénon map [16] is a well studied two dimensional iterative dynamical system, given by the following equa-

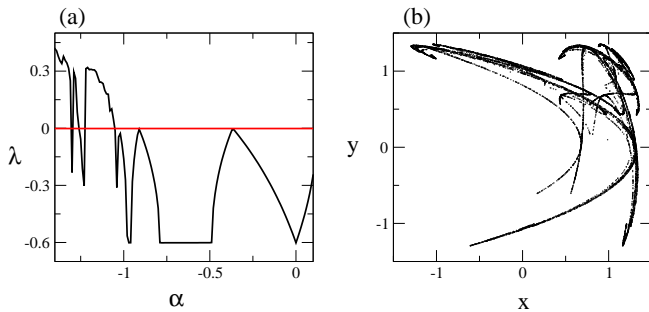


FIG. 1: (a) Variation of the Lyapunov exponent with  $\alpha$  at  $\beta = 0.3$  for the unmodulated Hénon map. (b) Aperiodic nonchaotic orbit in the Hénon map, parametrically modulated through an AFSR of order  $N=24$ . The attractors are obtained for parameter switching between  $\alpha = -0.14$  and  $\alpha = -1.2$ . The largest Lyapunov exponent is  $\lambda_1 = -0.16$ . The recurrence time for the AFSR is  $2^{24} - 1$ .

tions

$$x_{n+1} = 1 + \alpha x_n^2 + y_n, \quad (5)$$

$$y_{n+1} = \beta x_n. \quad (6)$$

For certain choice of  $(\alpha, \beta)$  and for a certain range of initial condition, the system exhibits chaotic or fixed point or periodic behaviour (see Fig. 1a).

Applying the strategy discussed above produces attractors which are both nonchaotic and essentially strange. In the Hénon map, at  $\alpha = -1.2$  the dynamics is chaotic and at  $\alpha = -0.14$  the dynamics goes to a fixed point (see Fig. 1a). Combining Eq. (4) and Eqs. (5-6), we get the following equations for the drive-response system

$$x_{n+1} = 1 + \alpha(1 + cz_n)x_n^2 + y_n, \quad (7)$$

$$y_{n+1} = \beta x_n, \quad (8)$$

$$z_{n+1} = \frac{1}{2} \left[ 1 - \cos\left(\pi \sum_{i=1}^N a_i z_{n+1-i}\right) \right]. \quad (9)$$

If we choose  $\alpha = -0.14$ ,  $\beta = 0.3$  and  $c = \frac{53}{7}$ , then depending on whether  $z_n$  is 0 or 1, the quantity  $\alpha(1 + cz_n)$  will take values of either  $-0.14$  or  $-1.2$ . As a result the dynamics hops between two different states such that the global dynamics is stable and nonchaotic. The Lyapunov exponent for the global dynamics is given by  $\lambda = -0.16$ . Fig. 1(b) shows the attractor in phase space. Clearly the attractor looks geometrically strange; the dynamics is aperiodic and nonchaotic.

## B. Lorenz system

The same strategy can be applied to a flow: switching the dynamics between a fixed-point or limit-cycle and a chaotic attractor can result in such strange dynamics in

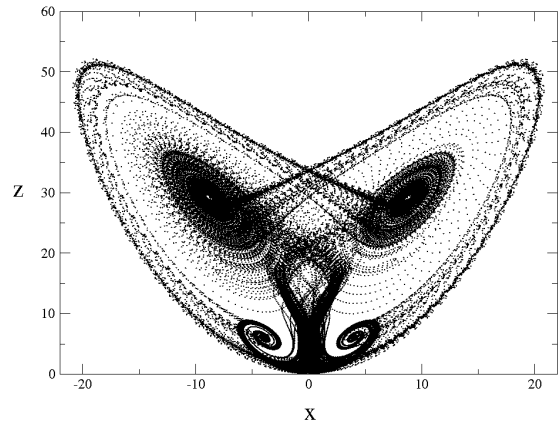


FIG. 2: Aperiodic nonchaotic attractor obtained in the phase-space for the Lorenz system under the AFSR modulation. Dynamics obtained for parameter values  $\rho = 7$  and  $c = \frac{23}{7}$  such that  $\rho$  switches between the values 7 and 30. Switch duration time is chosen to be  $\tau = 10$ , and the largest Lyapunov exponent is  $\lambda_1 = -0.00985$ .

a modulated Lorenz system [17],

$$\dot{x} = \sigma(y - x), \quad (10)$$

$$\dot{y} = (1 + c\zeta(t))\rho x - y - xz, \quad (11)$$

$$\dot{z} = xy - \beta z. \quad (12)$$

which has the parameter  $\rho$  changing in a time-dependent manner through the variable  $\zeta$ ,

$$\zeta(t) = z_n \quad n\tau \geq t \geq (n-1)\tau. \quad (13)$$

As in the mapping in Sec II A above,  $z_n$  is the output of an AFSR (Eq. 4) and the switch duration  $\tau$  is an additional parameter in the problem: it is the time for which a trajectory is switched into either of the states. In the present problem we have taken  $\tau$  to switch into either of the states to be equal, but one can choose mismatched  $\tau$ 's.

The attractor shown in Fig. 2 is the result of the dynamics hopping between parameter values  $\rho = 7$  and  $\rho = 30$ . At the latter value the attractor is chaotic with the characteristic butterfly structure about two symmetric unstable fixed points  $\{-8.79, -8.79, 29\}$  and  $\{8.79, 8.79, 29\}$ . For  $\rho = 7$  the system has two symmetrical attractive fixed points at  $\{-4, -4, 6\}$  and  $\{4, 4, 6\}$ . When the parameter switches between the values, the dynamics alternates between the stable and the unstable fixed point dynamics, resulting in the structure visible in Fig. 2.

## III. CHAOTIC MODULATION

A sequence generated from a chaotic signal can also generate aperiodic nonchaotic dynamics. For instance,

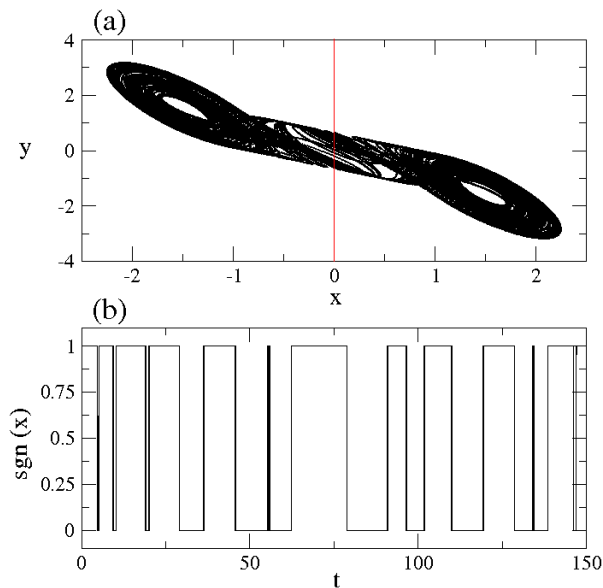


FIG. 3: (a) The Chua double-scroll attractor in the  $x - z$  plane. The fixed parameter values are  $c_1 = 9$ ,  $c_3 = 0$ ,  $m_0 = -\frac{8}{7}$ ,  $m_1 = \frac{5}{7}$ . The double-scroll is obtained by tuning the parameter  $c_2$ . Here we take  $c_2 = 14.141$ . (b) Corresponding bit sequence obtained assigning all points with positive value of  $x$  as ‘1’ and with negative values as ‘0’.

consider the Chua oscillator [18] which is described by the following sets of equations

$$\dot{x} = c_1(y - x - g(x)), \quad (14)$$

$$\dot{y} = x - y + z, \quad (15)$$

$$\dot{z} = -c_2y - c_3z, \quad (16)$$

where  $g(x)$  is given by,

$$m_1x + m_1 - m_0 \quad \text{if } x \leq -1, \quad (17)$$

$$g(x) = m_0x \quad \text{if } -1 \leq x \leq 1, \quad (18)$$

$$m_1x + m_0 - m_1 \quad \text{if } 1 \leq x. \quad (19)$$

For certain choice of the parameter  $c_3$ , a chaotic “double scroll” attractor is obtained (see Fig. 3a). We extract an indicator sequence of binary numbers from this chaotic attractor (see Fig. 3b) using the prescription that whenever the trajectory is on the left (resp. right) scroll, the indicator sequence is taken as 1 (resp. 0).

This gives a drive signal which is piecewise constant, which upon application to the Lorenz system discussed in Sec II B yields an attractor (see Fig. 4) that is very similar to that obtained via deterministic dichotomous driving. The main feature that both these drive signals share is that they have long periods when the drive is on the stable attractor, and this suffices to ensure that the eventual dynamics is aperiodic, and that the attractor has a complicated geometry and a nonpositive largest Lyapunov exponent.

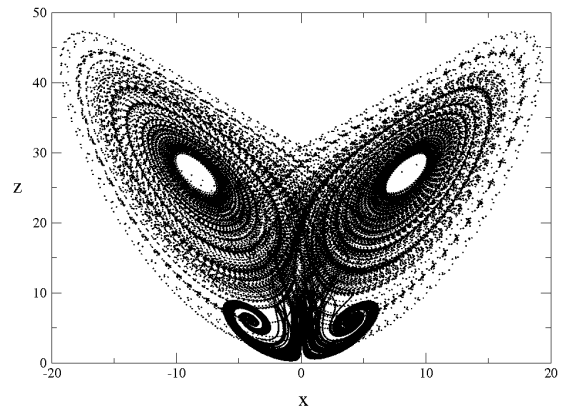


FIG. 4: Aperiodic nonchaotic attractors obtained in the phase-space for the Lorenz system using chaotic bit sequence from the Chua double scroll. The parameter values are  $\rho = 7$  and  $c = \frac{21}{7}$  such that  $\rho$  switches between the values 7 and 28. Switch duration time  $\tau$  is chosen to be unity. The largest LE is  $\lambda_1 = -0.03$ . The other parameters  $\sigma$  and  $\beta$  have values 10 and  $\frac{8}{3}$  respectively.

In the following section, we characterize these attractors via measures used in the study of SNAs.

#### IV. CHARACTERIZATION OF ANAS

Computation of the largest Lyapunov exponent shows that these attractors are nonchaotic. However, since the attractors are geometrically strange only over finite resolution, they differ in the qualitative and quantitative aspects of their local fluctuation properties [19] from other similar attractors such as SNAs.

Finite-time Lyapunov exponents (FTLES) [20] are local estimates for the rate of divergence between nearby trajectories, and explicitly depend both on the time interval  $\tau$  over which they are measured as well as the initial conditions. By computing  $\lambda_\tau$  for a large number of initial points in the phase space, one can obtain the stationary distribution,

$$P(\lambda, \tau) = \text{Probability that } \lambda_\tau \quad (20)$$

$$\text{lies in the interval } (\lambda, \lambda + d\lambda). \quad (21)$$

For SNAs this is typically broad and non-Gaussian [19, 21, 22], although the mean of the distribution, namely the asymptotic Lyapunov exponent, is negative.

The FTLE distribution for ANAs is purely Gaussian: see Figs. 5((a) and (b)) for the driven Hénon and Lorenz systems. This follows from the pseudo-random nature of the driving which switches the dynamics between a regular and a chaotic state. Correlations die out rapidly and the FTLEs satisfy the central limit theorem. As a result the distribution is a Gaussian whose spread is a function of the length of the trajectory [19].

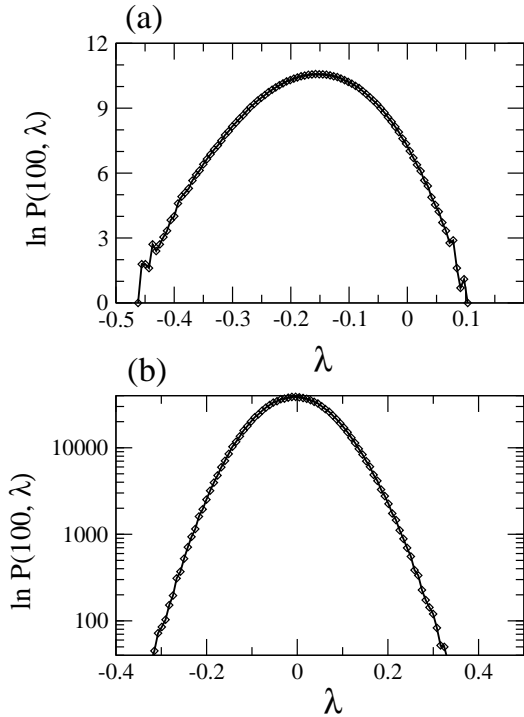


FIG. 5: Finite time Lyapunov exponent (FTLE)s. (a) for the modulated Hénon map with parameter values  $\alpha = -0.14$  and  $c = \frac{53}{7}$ . Asymptotic largest LE value is  $\lambda_1 = -0.16$ . The distribution is taken for  $N = 100$ . (b) Similar results for the modulated Lorenz system with parameter values as in Fig 2 and asymptotic largest LE is  $\lambda_1 = -0.00985$ .

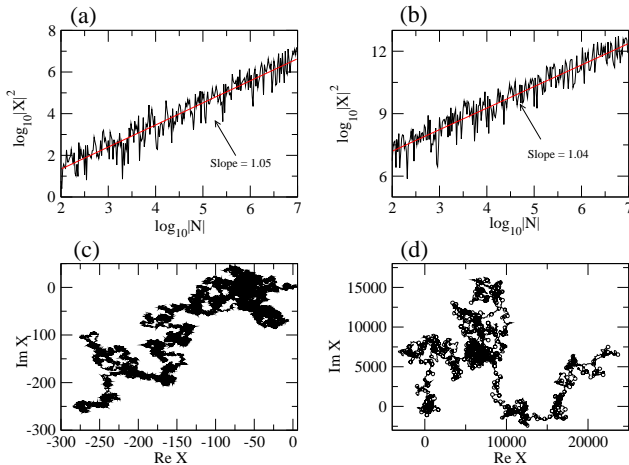


FIG. 6: Finite-time Fourier power  $|X(\Omega, N)|^2$  versus  $T$  on a logarithmic scale for (a) the Hénon map, and (b) the Lorenz system. Fractal walk of the spectral trajectory in the complex plane ( $\text{Re}X$ ,  $\text{Im}X$ ) for (c) the Hénon map, and (d) for the Lorenz system. Parameter values are as in Fig. 1(a) and Fig. 2.

The contrast between ANAs and SNAs is also evident in the Fourier spectrum [23]. Upon computing the time-dependent partial Fourier sum [2, 23]

$$X(\Omega, N) = \sum_{n=1}^N x_n \exp^{i2\pi n\Omega}, \quad (22)$$

at irrational frequency  $\Omega$  the golden mean ratio,  $(\sqrt{5} - 1)/2$ , the scaling relation  $|X(\Omega, N)|^2 \sim N^\beta$  is observed. For noisy motion,  $\beta = 1$ , and the spectrum is continuous. For periodic motion  $\beta = 2$  and the spectrum is discrete. For singular continuous spectrum (as in SNAs [23]) the scaling exponent satisfies  $1 < \beta < 2$  [23]. Here we find that the Fourier sum obeys scaling, with an exponent slightly greater than unity; see Figs. 6((a) and (b)). This implies that the dynamics in these attractors is typically noisy unlike SNAs where the dynamical correlation persists over long times due to intermittency. For non-chaotic attractors in the Hénon and the Lorenz systems, we find the exponents  $\beta = 1.05$  and  $\beta = 1.04$  respectively. Fig. 6((c) and (d)) shows the respective spectral trajectories in the complex plane ( $\text{Re} X, \text{Im} X$ ).

A detailed characterization of the nature of dynamics can be obtained from measures based on recurrences [24]. Recurrence plots (RPs) are defined for a given trajectory  $\{\vec{x}_i\}_{i=1}^N$  through the matrix

$$R_{i,j} = \Theta(\delta - \|\vec{x}_i - \vec{x}_j\|), \quad i, j = 1, \dots, N \quad (23)$$

where  $\delta$  is a predefined threshold,  $\Theta(\cdot)$  the Heaviside function and  $\|\cdot\|$  the maximum norm. The maximum norm (also called infinity norm) of a vector  $\vec{x}$  of length  $N$  is given by  $\|\vec{x}\|_\infty = \max(|x_1|, \dots, |x_N|)$ . Points that are closer (respectively further) than  $\delta$  yield an entry “1” (respectively “0”) in the matrix  $R_{i,j}$ . Then, the values “1” and “0” are depicted as black and white dot in a two-dimensional plot, providing a visual representation of the system dynamics. The RPs exhibit characteristic large scale and small scale patterns (called *typology* and *texture* respectively); these have been comprehensively reviewed recently [25]. The selection criteria for the threshold  $\delta$  is discussed in details in a review by Marwan *et al.* [25]. Here we take  $\delta$  in units of the standard deviation  $\sigma$  of the trajectory.

In Fig. 7, we compare the RPs for a SNA in the quasiperiodically forced Hénon map [27] and the ANA for the modulated Hénon map. It is clear that the RP of ANA (Fig. 7(b),(d)) consists of more isolated correlated points and short diagonal segments depicting short-range correlations. On the other hand, the RP for SNA (Fig. 7(a),(c)) has a larger distribution of longer diagonal line segments implying that correlation persists over long times – a signature of quasiperiodic driving.

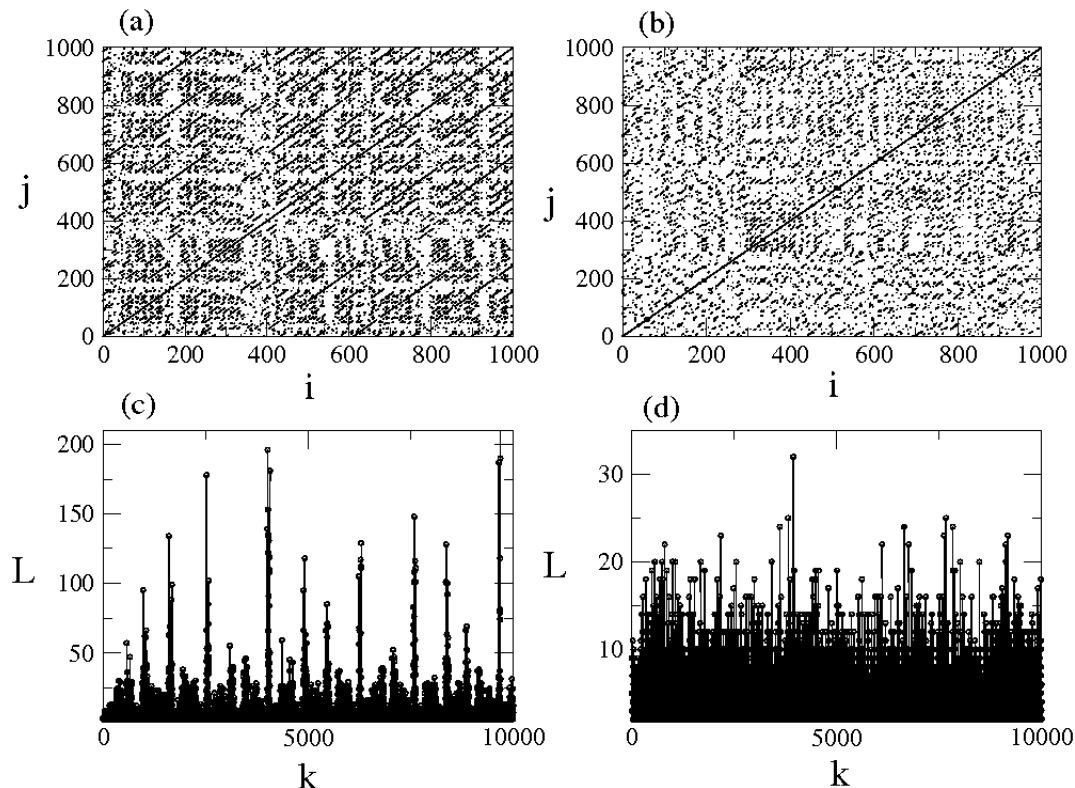


FIG. 7: Comparison of recurrence plots for (a) a strange nonchaotic attractor for the quasiperiodically forced Hénon map [27], and, (b) the aperiodic nonchaotic attractor for the driven Hénon map with parameters as given in Fig. 1(b). The RP for SNA has longer diagonal length segments due to long range correlations as compared to that of the ANA which consists of more isolated correlated points and shorter diagonal length segments. This is seen in (c) and (d) where the diagonal length distribution (with minimum length  $L_{min} = 2$  in each case) for the two cases are compared. We calculated the *determinism* ( $DET$ ) for both the cases (see Eq. 46 in Marwan *et al.* [25]) and for SNA,  $DET = 0.78$ , whereas for ANA it is  $DET = 0.62$ . Here we take  $\delta = 0.3\sigma$  where  $\sigma$  is the standard deviation of the trajectory.

## V. EXPERIMENT

In the electronic experiments reported here we have designed a circuit that essentially obeys the Lorenz equations [17] and permits one of the parameters to be switched between two values.

The typical parameters for the butterfly attractor are  $\sigma = 10$ ,  $b = 8/3$  and in our circuit the value of  $\rho$  may be switched between 28 and 7 (as in Fig. 4). The switching of  $\rho$  is controlled by a chaotic pulse generated from a Chua circuit [28, 29]:  $\rho = 28$  if the drive signal has value 1, else  $\rho = 7$  (and the drive signal has the value 0). The experimental circuit of the pulse driven Lorenz oscillator is shown in Fig. 8. A Chua circuit is designed using two op-amps (U1-U2:  $\mu 741$ ), capacitors C1 and C2, inductor L1 with a leakage resistance R8 and other resistances R1-R7. It generates a chaotic double scroll for choice components noted in the circuit diagram. The dynamics of the Chua circuit can be controlled by varying R1 resistance keeping other components fixed. The double-scroll chaos from the Chua circuit is then applied

to a Schmitt trigger circuit designed by using op-amp U3, an inverting amplifier U4 and associated resistances R9-R13. The output from U3 and U4 are used to control the analog switches U5A and U6A respectively to allow continuity of either R16 or R17 in the Lorenz circuit. The Lorenz circuit is implemented using two analog multipliers U7-U8, and three op-amps (U9-U11:  $\mu 741$ ), capacitors C3-C5 and resistances R14-R21. The choice of resistances R16 and R17 made the selection of  $\rho$ -value between 7 ( $= R19/R16$ ) and 28 ( $= R19/R17$ ) respectively. The other parameter of the Lorenz circuit are decided as  $\sigma = R19/R14$  and  $b = R19/R21$ . The analog switches are in ON state if their control pulse at VC terminal is positive. So the analog switch U5A is in ON state when the output of U3 is positive but U6A is in OFF state.

Alternately, the analog switch U6A is in ON state and U5A is in OFF state when the output of U3 is negative but inverted by the U4 to make the control pulse positive at the VC terminal of U6A. The oscilloscope picture of the control pulse as generated from the Chua circuit is shown in Fig. 9. The upper trace is the double scroll chaotic signal from the Chua circuit which is processed

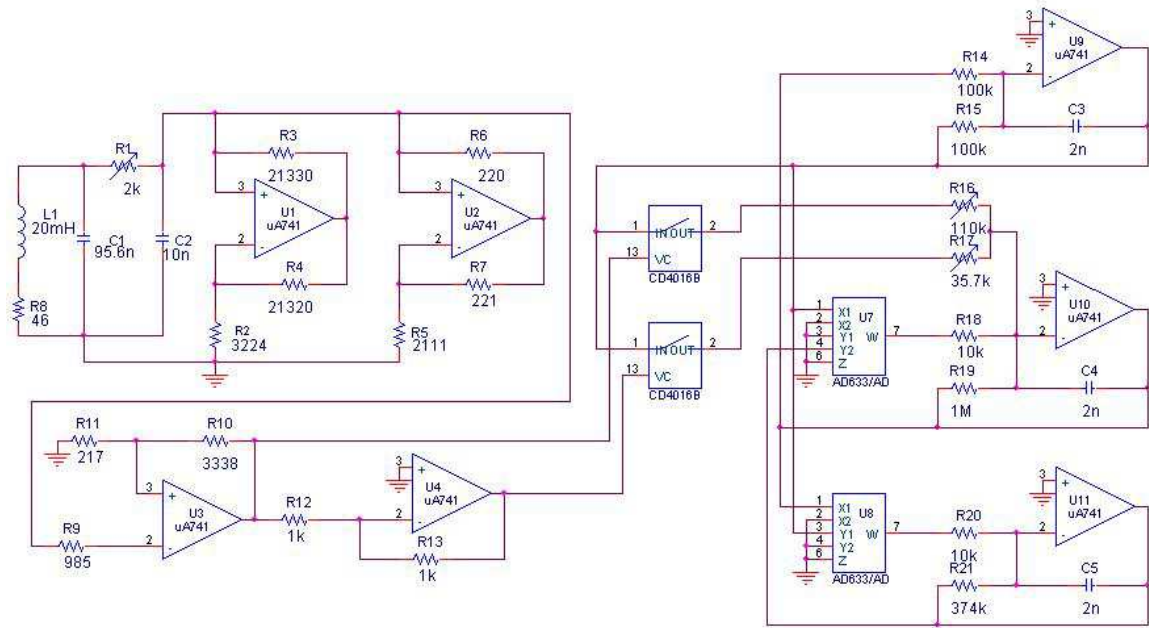


FIG. 8: (Colour Online) Experimental Lorenz circuit: ICs (U1-U8) power supply  $\pm 9V$ olt and (U9-U11) power supply  $\pm 15$  Volt. All resistances are in Ohms.

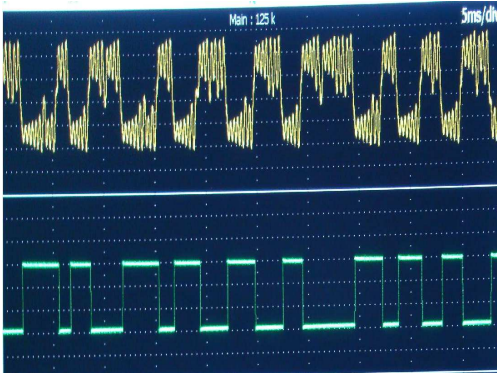


FIG. 9: (Colour Online) Chaotic pulse generated using Chua oscillator: upper trace is the chaotic voltage  $VC_2$  at capacitor node C2 of the Chua circuit and the lower trace is the voltage measured at the output of the op-amp U3. Upper trace is scaled-up and the lower trace is scaled-down for visual clarity.

by the Schmitt trigger U3. The chaotic pulse is clearly seen in the lower trace as switching between a positive and a negative value almost randomly; the signal is scaled down in the oscilloscope.

The chaotic control signal switches the  $\rho$ -value of the Lorenz circuit aperiodically. The phase portrait of the Lorenz circuit is shown in Fig. 10: this is the ANA that results from the theoretical strategy outlined in Sec III; see Fig. 4.

To show that the attractors obtained experimentally satisfy the synchronization condition, we constructed an

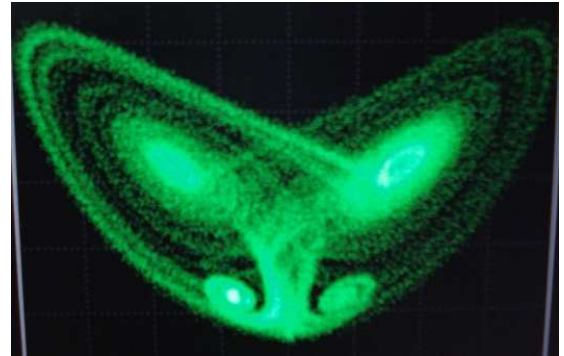


FIG. 10: (Colour Online) Oscilloscope picture of the ANAs in the modulated Lorenz circuit: output voltage of U8 plotted against the output voltage of U11.

auxiliary system [30]. Two identical Lorenz oscillators are controlled by the chaotic pulse generated from a single Chua oscillator. The components of the Lorenz oscillators are carefully chosen with 1% tolerance so that both the oscillators are almost identical. Synchronization of two the nonchaotic Lorenz circuit is now investigated, the circuit scheme of which is shown in Fig. 11. We observe that the output voltage of the Lorenz oscillators, OS-1 and OS-2, are completely synchronized. The oscilloscope pictures of the two time series from the oscillators are shown in green and blue in Fig. 12 for comparison. The time series plotted one against the other, is shown as a thick line, confirms complete synchronization of the two oscillators (within experimental bounds). The width of

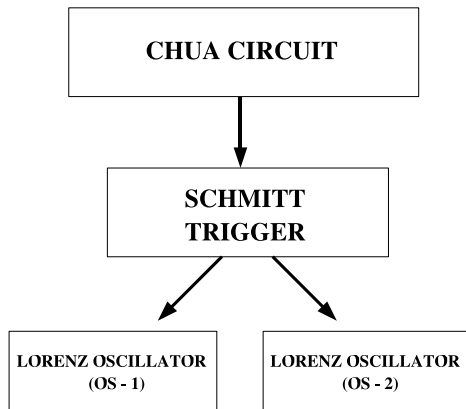


FIG. 11: Block diagram of a system of two Lorenz circuits modulated by the chaotic drive of a Chua circuit.

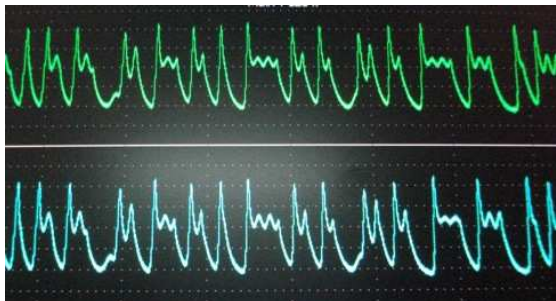


FIG. 12: (Colour Online) Oscilloscope picture of the output voltages showing the experimental time series of the two Lorenz circuits.

the synchronization manifold is due to natural parameter mismatch between the two designed Lorenz oscillators; this is unavoidable in experiments.

## VI. DISCUSSION

Motion that is both stable and aperiodic is ubiquitous in natural systems [1, 31]. The manner in which such dynamics can be created is therefore of interest. One class of attractors that have these features has been known for some time now, but a quasiperiodic drive is essential for their creation [2] and thus these appear to be somewhat exceptional. An area where these considerations are potentially important is in the dynamics of biological systems. Although not manifestly periodic, several bio-

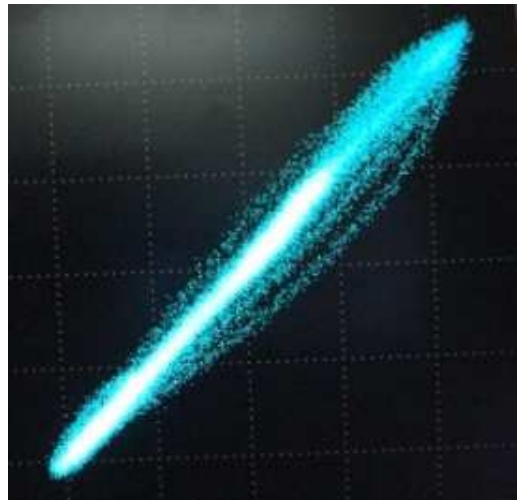


FIG. 13: (Colour Online) Oscilloscope picture of synchronization: similar output signals as shown in Fig. 11 measured from two Lorenz circuits are plotted against each other to draw the synchronization manifold.

logical phenomena are stable, at least in a homeostatic sense [31, 32]. Thus it is a moot question whether aperiodic but nonchaotic attractors are responsible for such stability.

On SNAs there is a delicate balance between global stability: as was established by Sturman and Stark [33] there is an unstable set embedded within the attractor. The design strategy that we have enunciated in the present work keeps this feature in mind: the scheme we have proposed here is to modulate system parameters in such a manner as to achieve global stability while ensuring local instability.

This method of dichotomous modulation creates attractors which are nonchaotic and have a fractal geometry on experimentally accessible timescales. We have recently shown [34] that SNAs created via quasiperiodic forcing are a manifestation of weak generalized synchronization, and that similar stable attractors can be created by chaotic forcing [34]. The parametric modulation used in the present case retains the skew-product structure of the dynamical system. The formation of these stable attractors can in some sense be seen as an instance of generalized synchronization [30].

The attractors created via such parameter modulation are quite distinct from SNAs. The Gaussian nature of the FTLE distribution shows that the dynamics is not intermittent. From the spectral properties it is evident that unlike SNAs, the power spectrum varies as  $|X(\Omega, N)|^2 \sim N$ , which occurs when the motion is random or chaotic. Our system being nonchaotic, the randomness in the motion comes from the stochastic nature of the modulation. This is confirmed by looking at the correlation properties via recurrence plots, which shows similar behaviour to that of random or chaotic dynamics.

The aperiodic nonchaotic attractors can be realized in an experimental setup. As an example, we construct an electronic circuit experiment wherein a Chua double scroll attractor is used to drive a Lorenz attractor. The experiment closely matches the simulation result, and by experimentally constructing an auxiliary system [35] we demonstrate that for a given drive sequence, trajectories with different initial states synchronize rapidly on the ANAs. This demonstrates the possibility of creating—or using—such dynamics in practical applications [36]. Fur-

thermore such a realization shows the robustness of the proposed design scheme against external noise.

### Acknowledgments

S.K.D. and S.K.B. acknowledges support by the DST, India under grant #SR/S2/HEP-03/2005.

- 
- [1] A. Prasad, A. Nandi and R. Ramaswamy, *Int J. Bifurcation and Chaos* **17**, 3397 (2007).
- [2] A. Prasad, S. S. Negi and R. Ramaswamy, *Int J. Bifurcation and Chaos* **11**, 291 (2001).
- [3] C. Grebogi, E. Ott, S. Pelikan and J. A. Yorke, *Physica D* **30**, 261 (1984).
- [4] R. Ramaswamy, *Phys. Rev. E* **56**, 7294 (1997).
- [5] W. L. Ditto et al, *Phys. Rev. Lett.* **65**, 533 (1990).
- [6] S. Rajasekar, *Phys. Rev. E* **51**, 775 (1995).
- [7] V. S. Anishchenko, T. E. Vadivasova and O. Sosnovtseva, *Phys. Rev. E* **54**, 3231 (1996).
- [8] A. S. Pikovsky, M. A. Zaks, U. Feudel and J. Kurths, *Phys. Rev. E* **52**, 285 (1995).
- [9] X. Wang, M. Zhan, C. H. Lai and Y. C. Lai, *Phys. Rev. Lett.* **92**, 074102 (2004).
- [10] A. Prasad and R. Ramaswamy *Proc. Ind. Natl. Sci. Acad.*, p. 859, (2000).
- [11] R. Roy, T. W. Murphy, T. D. Maier Jr., Z. Gills and E. R. Hunt, *Phys. Rev. Lett.* **68**, 1259 (1992).
- [12] S. Rajasekhar, M. C. Valsakumar and S. P. Raja *Physica A* **261**, 417 (1998).
- [13] I. Broussell, I. L'Heureux and E. Fortin, *Phys. Lett. A* **225**, 85 (1997).
- [14] M. K. Simon, *et al.*, *Spread Spectrum Communications Handbook* (McGraw-Hill, New York, 1994).
- [15] N. Gershenfeld and G. Grinstein *Phys. Rev. Lett.* **74**, 5024 (1995).
- [16] M. Hénon, *Comm. Math. Phys.* **50**, 69 (1976).
- [17] E. Lorenz, *J. Atmos. Sci.* **20**, 130 (1963).
- [18] T. Matsumoto, L. O. Chua and M. Komuro, *IEEE Trans. Cir. Sys.*, **23**, 798, (1985).
- [19] A. Prasad and R. Ramaswamy, *Phys. Rev. E* **60**, 2761 (1999).
- [20] H. D. I. Abarbanel, R. Brown and M. B. Kennel, *J. Nonlin. Sci.* **2**, 343 (1991).
- [21] A. Pikovsky and U. Feudel, *Chaos* **5**, 253 (1995).
- [22] A. Prasad, V. Mehra and R. Ramaswamy, *Phys. Rev. E* **57**, 1576 (1998).
- [23] A. Pikovsky and U. Feudel, *J. Phys. A* **27**, 5209 (1994).
- [24] J. P. Eckmann, S. O. Kamphorst and D. Ruelle, *Europhys. Lett.* **4**, 973 (1987).
- [25] N. Marwan, M. C. Romano, M. Thiel and J. Kurths, *Phys. Rev.* **438**, 237 (2007).
- [26] E. J. Nganga, A. Nandi, R. Ramaswamy, M. C. Romano, M. Thiel, and J. Kurths, *Phys. Rev. E* **75**, 036222 (2007).
- [27] O. Sosnovtseva, U. Feudel, J. Kurths and A. Pikovsky *Phys. Lett. A* **218**, 255 (1996).
- [28] M.P Kennedy, *IEEE Trans. Cir. Sys.*-I, **47**, 76, (2000).
- [29] S.K.Dana, B. Blasius and J. Kurths, *Chaos* **16**, 023111 (2006).
- [30] H. D. I. Abarbanel, N. F. Rulkov and M. M. Sushchik, *Phys. Rev. E* **53**, 4528 (1996).
- [31] L. Glass, *Nature* **410**, 277 (2001).
- [32] M. G. Vilar, H. Y. Kueh, N. Barkai and S. Leibler, *Proc. Natl. Acad. Sci. (USA)* **99**, 5988 (2002).
- [33] R. Sturman and J. Stark, *Nonlinearity* **13**, 113 (2000).
- [34] T. U. Singh, A. Nandi and R. Ramaswamy *Phys. Rev. E* **78**, 025205(R) (2008).
- [35] H. D. I. Abarbanel, N. F. Rulkov, and M. M. Sushchik, *Phys. Rev. E* **53**, 4528 (1996).
- [36] K. M. Cuomo and A. V. Oppenheim, *Phys. Rev. Lett.* **71**, 65 (1993); R. Ramaswamy, *Phys. Rev. E* **56**, 7294 (1997); C. Zhou and T. Chen, *Europhys. Lett.* **38**, 261 (1997); H.L. Yang, *Phys. Rev. E* **63**, 036208 (2001).